Fluorescence and Absorption Spectroscopy of the Weakly Fluorescent Chlorophyll *a* in Cytochrome b_6f of *Synechocystis PCC6803*

Erwin J. G. Peterman,* Stephan-Olav Wenk,# Tõnu Pullerits,§ Lars-Olof Pålsson,* Rienk van Grondelle,* Jan P. Dekker,* Matthias Rögner,# and Herbert van Amerongen*

*Department of Physics and Astronomy and Institute for Molecular Biological Sciences, Vrije Universiteit, 1081 HV Amsterdam, the Netherlands; #Lehrstuhl für Biochemie der Pflanzen, Ruhr Universität, D-44780 Bochum, Germany; and §Department of Chemical Physics, Chemical Center, Lund University, Lund, Sweden

ABSTRACT A spectroscopic characterization of the chlorophyll *a* (Chl) molecule in the monomeric cytochrome b6f complex ($Cytb_6f$) isolated from the cyanobacterium *Synechocystis PCC6803* is presented. The fluorescence lifetime and quantum yield have been determined, and it is shown that Chl in $Cytb_6f$ has an excited-state lifetime that is 20 times smaller than that of Chl in methanol. This shortening of the Chl excited state lifetime is not caused by an increased rate of intersystem crossing. Most probably it is due to quenching by a nearby amino acid. It is suggested that this quenching is a mechanism for preventing the formation of Chl triplets, which can lead to the formation of harmful singlet oxygen. Using site-selected fluorescence spectroscopy, detailed information on vibrational frequencies in both the ground and Q_y excited states has been obtained. The vibrational frequencies indicate that the Chl molecule has one axial ligand bound to its central magnesium and accepts a hydrogen bond to its 13^1-keto carbonyl. The results show that the Chl binds to a well-defined pocket of the protein and experiences several close contacts with nearby amino acids. From the site-selected fluorescence spectra, it is further concluded that the electron-phonon coupling is moderately strong. Simulations of both the site-selected fluorescence spectra and the temperature dependence of absorption and fluorescence spectra are presented. These simulations indicate that the Huang-Rhys factor characterizing the electron-phonon coupling strength is between 0.6 and 0.9. The width of the Gaussian inhomogeneous distribution function is 210 $\pm$ 10 cm^{-1}.

INTRODUCTION

In organisms that perform oxygenic photosynthesis, the cytochrome b6f complex ($Cytb_6f$) is the redox complex that couples the two photosystems. It accepts electrons from photosystem II via plastoquinol and transfers these to photosystem I via plastocyanin (or cytochrome c553 in some cyanobacteria) (Cramer et al., 1996; Hauska et al., 1996). The complex is related in structure and function to the cytochrome bc1 complex of bacteria and mitochondria, in which it is a key redox complex in the respiratory chain (Cramer et al., 1996; Xia et al., 1997). In fact, in cyanobacteria, $Cytb_6f$ also functions in respiration (Hauska et al., 1996). The complex consists of four redox cofactors: a c-type heme, bound by the cytochrome f protein; two b-type hemes, bound by the cytochrome b6 protein; and a 2Fe-2S cluster, bound by the Rieske Fe-S-protein (Hauska et al., 1996). Apart from the three redox-cofactor-binding proteins, an additional larger subunit (subunit IV) and several small subunits are part of the complex (Cramer et al., 1996). $Cytb_6f$ can be isolated as a dimer, which is believed to be the active form (Huang et al., 1994; Breyton et al., 1997), or as a monomer, which usually lacks the Rieske Fe-S-protein (Bald et al., 1992; Breyton et al., 1997).

A surprising finding was that isolated $Cytb_6f$ from different species (spinach (Huang et al., 1994), the unicellular alga *Chlamydomonas reinhardtii* (Pierre et al., 1995, 1997), and the cyanobacterium *Synechocystis PCC6803* (Bald et al., 1992)) binds a chlorophyll *a* (Chl *a*) molecule. For the complex from *C. reinhardtii*, it has been convincingly shown that this Chl is an intrinsic component of the complex and not a contamination (Pierre et al., 1997). The Chl molecule has been characterized by absorption, emission, and resonance Raman spectroscopy (Pierre et al., 1997). It was shown that the fluorescence yield (at 77 K) was about four times lower than that of Chl *a* in vitro. The resonance Raman spectra showed a single population of Chl, hydrogen bonded to the protein via the 13^1-keto carbonyl. This indicates that the Chl is bound to a single, specific binding pocket. The ligation state of the central Mg could not be determined unambiguously (Pierre et al., 1997). Recent experiments indicate that the Chl is bound to the cytochrome b6 protein (Poggese et al., 1997). Several ideas about the functions of the Chl molecule in the complex have been put forward, but it was concluded that the most likely explanation is that the Chl is an evolutionary relic (Pierre et al., 1997).

Here we present a study of the spectroscopic properties of the Chl molecule in the $Cytb_6f$ complex of the cyanobacterium *Synechocystis PCC6803*. An important question we will address is the fate of excited states of this Chl. Isolated Chl has a high quantum yield (~60%) of intersystem crossing to the triplet state. Triplet excited Chl can transfer its excitation energy to oxygen. In this process oxygen is

Received for publication 20 November 1997 and in final form 8 April 1998.

Address reprint requests to Dr. Herbert van Amerongen, Free University of Amsterdam, Department of Biophysics, Faculty of Physics and Astronomy, De Boelelaan 1081, 1081 HV Amsterdam, the Netherlands. Tel.: +31-20-4447932; Fax: +31-20-4447899; E-mail: herbert@nat.vu.nl.

Dr. Peterman's present address is Department of Chemistry and Biochemistry, University of California–San Diego, La Jolla, CA 92093-0340.

0006-3495/98/07/389/10 $2.00

sensitized to its singlet excited state (Siefermann-Harms, 1987). Singlet oxygen is a reactive oxidizing agent that is toxic to the organism. Efficient protection against the harmful effects of singlet oxygen is essential and is mostly realized by carotenoids, which can quench Chl triplet states (Siefermann-Harms, 1987). In this respect it is interesting to find out how the problem of Chl triplet states is dealt with in $Cytb_6f$.

Another interesting aspect of the Chl in $Cytb_6f$ is that it is a relatively simple (with respect to interaction with other Chl's), naturally occurring model system for Chl in a protein environment. In general, the Q_y absorption band of Chl in a protein environment is inhomogeneously broadened. The relatively broad, structureless absorption band is a convolution of the inhomogeneous distribution function (IDF), which describes the distribution of the absorption maxima of the individual pigments, and the single-site absorption spectrum (Personov, 1983; Avarmaa and Rebane, 1985). This single-site absorption spectrum can be quite structured and consists of a sharp line, the zero-phonon line (ZPL), and a broader wing to the blue, the phonon wing (PW). The ZPL is due to a purely electronic transition. The width of the ZPL is determined by the dephasing and decay times of the excited electronic state (Avarmaa and Rebane, 1985). The PW is due to a combined electronic and phonon transition. In a protein environment, phonons are due to collective vibrations of (part of) the protein in which the pigment is embedded. The shape and relative intensity of the PW are determined by the phonon density of states and the strength of coupling between electronic and phonon transitions (Pullerits et al., 1995). The temperature-dependent population of the phonon energy levels is responsible for the broadening of the absorption band with increased temperature (Pullerits et al., 1995). In general, a single-site absorption spectrum also consists of "replicas" (to the blue) of these ZPLs and PWs due to vibronic transitions. The sharp vibronic ZPLs (vZPLs) present in these spectra are separated from the purely electronic ZPL by the vibrational frequency (Personov, 1983; Pullerits et al., 1995). In the case of Chl, these vibrational frequencies contain detailed information on the exact binding (one or two axial ligands, the presence of hydrogen bonds) of the Chl to the protein (Lutz and Robert, 1988). The absorption properties mentioned above are also present in fluorescence (when mirrored on an energy scale). We will present high-resolution fluorescence measurements and simulations as performed before on light-harvesting complex II (LHCII) (Peterman et al., 1997) and the reaction center of photosystem II (Peterman et al., in press), both from green plants. These measurements and simulations provide detailed information on electron-phonon and vibronic coupling of Chl in $Cytb_6f$.

MATERIALS AND METHODS

Sample preparation

The purification procedure and the characterization of the $Cytb_6f$ from *Synechocystis PCC6803* will be described in detail elsewhere. In short, a glucose-tolerant strain of *Synechocystis PCC6803* lacking photosystem I (a kind gift of Dr. W. F. J. Vermaas, Arizona State University, Tempe, AR) was photoheterotrophically grown in a 25 liter carboy in the presence of 30 mM glucose. The cells were harvested and thylakoid membranes were prepared as described by Rögner and co-workers (Rögner et al., 1990). Cyt b6f was extracted from the thylakoids by incubation with 1% (w/v) *n*-dodecyl-β,D-maltoside (DM) for 30 min at room temperature. After centrifugation (40,000 rpm, 1 h, 4°C, Sorvall T 647.5 rotor), Cyt b6f was purified from the supernatant by applying two high-performance liquid chromatography perfusion chromatography steps. The buffer composition of the final complex was 20 mM 2-(*N*-morpholino)ethanesulfonic acid (MES) (pH 6.5), 10 mM $CaCl_2$, 10 mM $MgCl_2$, 5 mM $MgSO_4$, 0.5 M mannitol, and 0.03% (w/v) DM. Characterization by sodium dodecyl sulfate-polyacrylamide gel electrophoresis revealed the presence of Cyt f (29 kDa), Cyt b6 (22 kDa), subunit IV (17 kDa), and two or three small subunits (4–6 kDa). Characterization by high-performance liquid chromatography–gel filtration chromatography (Bald et al., 1992) showed that the isolated complexes were essentially monomeric. The prepation lacks the Rieske protein, which was confirmed by immunoblotting (S. O. Wenk, unpublished results). The complex contains 1.07 Chl per Cyt f. This value was determined from the ratio of the absorption maxima at 556 nm for Cyt f (via the ascorbate-reduced minus ferricyanide-oxidized difference spectrum) and at 670 nm for Chl (corrected for baseline effects). Extinction coefficients of 26 mM^{-1} cm^{-1} for Cyt f (Metzger et al., 1997) and 75 mM^{-1} cm^{-1} for Chl (Dawson et al., 1986) were assumed.

For the measurements, the complex was dissolved in a buffer containing 20 mM MES-HCl (pH 6.5), 10 mM $MgCl_2$, 10 mM $CaCl_2$, and 0.05% DM. All experiments were perfomed on the air-oxidized complex, unless stated differently. The redox state of the complex was altered by the addition of ferricyanide (2 mM, to oxidize the f and both the b6 hemes), ascorbate (40 mM, to reduce the f-heme), and dithionite (100 mM, to also reduce both b6 hemes). Low-temperature experiments were performed in an Utreks helium bath cryostat (fluorescence), an Oxford Instruments helium flow (absorption), or a nitrogen bath cryostat (triplet-minus-singlet absorption difference (T-S) measurements).

Spectroscopic measurements

Absorption spectra were recorded on a Cary 219 spectrophotometer, with a spectral bandwidth of 1 nm. Fluorescence spectra were recorded as described previously (Peterman et al., 1997) with a CCD camera (Chromex Chromcam 1), via a 1/2-m spectrograph (Chromex 500IS). Excitation light was provided by a tungsten-halogen lamp via a bandpass filter, or a dye laser (Coherent CR599, dye DCM, spectral bandwidth 1 cm^{-1}) pumped by an Ar^+ laser (Coherent Inova 310). For the fluorescence measurements, an optical density (OD) of 0.1 in the Q_y maximum was used, unless stated otherwise. The power of the excitation laser was kept below 200 $\mu W/cm^2$, to minimize the effects of spectral hole burning. For the vibronically excited spectra, the power could be increased to 2 mW/cm^2. Fluorescence quantum yields were determined from the ratio of the areas of emission of $Cytb_6f$ and Chl *a* (Sigma) in methanol (fluorescence yield 22%; Seely and Connolly, 1986). The areas were corrected for the amount of absorbed photons at the excitation wavelength. Laser excitation was in the 660–680-nm range.

Time-resolved fluorescence measurements were performed on a synchroscan streak camera (Hamamatsu M5680). Excitation light pulses (wavelength 670 nm, duration ~150 fs, power 100 μW, repetition rate 250 kHz) were provided by a combination of a Coherent MIRA 900 Ti:sapphire oscillator, a RegA 9000 amplifier, and an OPA 9400 optical parametric amplifier. The instrument response was ~5 ps, the time base 800 ps, and the spectral range of detection 640–740 nm. The polarization of detection was at a magic angle relative to that of excitation. Data were deconvoluted and analyzed globally, using software (Van Stokkum et al., 1994) kindly provided by Dr. I. H. M. van Stokkum.

Chl T-S absorption transients were measured as described before (Groot et al., 1995). Excitation light with a wavelength of 590 nm was provided by a dye laser (Quanta Ray PDL2, pulse energy ~10 mJ, pulse duration ~6

ns) pumped by a Q-switched Nd:YAG laser (Quanta Ray DCR2). Changes in absorption of light provided by a tungsten-halogen lamp were measured with a silicon photodiode via a 1/4-m monochromator and digitized with a digital oscilloscope (LeCroy 9310). The time response of the setup was 10 μs. For the measurements of carotenoid triplets, a xenon lamp and a photomultiplier (Hamamatsu R928, time response <1 μs) were used.

RESULTS AND SIMULATIONS

Absorption spectra

In Fig. 1 the absorption spectrum of $Cytb_6f$ at 4 K is shown. The most intense transition in the spectrum (at 416 nm) is mainly due to the Soret bands of the hemes. The Q peaks of the hemes (in the region of 520–560 nm) are hardly visible, as expected for air-oxidized $Cytb_6f$. The peaks at 521 nm and 493 nm are most probably due to carotenoids (Cars), specifically or nonspecifically bound to the complex. Cars (mainly β-carotene) have also been identified in the $Cytb_6f$ of *C. rheinhardtii* (Pierre et al., 1995, 1997). The Chl in the complex shows a Q_y maximum at 670.5 nm. In the Q_x/vibronic Q_y region, peaks at 629, 619, and 611 nm can be observed. The shoulder at ~435 nm is due to the Soret transition of the Chl. In the inset, the Chl Q_y band is shown at several temperatures between 4 K and 275 K. At 4 K the spectrum peaks at 670.5, and at 275 K it peaks at 670 nm. The width (full width at half-maximum, FWHM) of the spectrum increases from 11.6 nm at 4 K to 16.2 nm at 275 K. Broadening of the Q_y absorption band has been explained in terms of the temperature-dependent population of phonon levels (Pullerits et al., 1995). Simulations of this phenomenon will be presented below.

Nonselective emission spectra

In Fig. 2 the emission spectrum of $Cytb_6f$ at 5 K is shown, obtained upon broad-band excitation at 455 nm. Because of a small contamination with strongly fluorescent phycobilisome proteins, we could only obtain "clean" Chl emission spectra upon (broad band) excitation below 500 nm. On the blue side of the spectrum of Fig. 2, a small background of phycobilisome protein emission is present. The spectrum is a typical Chl *a* emission spectrum, peaking at 678 nm, with a width of 15.3 nm (FWHM). We note that the nonselective emission is considerably broader than the absorption and that the Stokes shift (peak to peak) is rather large. Because of the relatively large width of the band, hardly any vibronic structure can be distinguished (compare this, for example, to the nonselectively excited spectrum of LHCII; Kwa et al., 1994). Also shown (in the inset) are the main peaks of the emission spectra at higher temperatures. As the temperature is increased, the spectrum becomes broader and shifts to the blue, and the integrated intensity decreases. At room temperature the spectrum peaks at 676.5 nm and has a width of 19.8 nm (FWHM). The temperature dependence of the width of the emission spectrum has the same cause as that of the width of the absorption spectrum: temperature-dependent population of the phonon levels (Pullerits et al., 1995) (see simulations below). The total intensity of the emission, which is proportional to the fluorescence quantum yield, decreases by a factor of 2, going from 5 K to room temperature. A comparable (45%) decrease in the quantum yield of Chl *a* fluorescence as the temperature is increased from 4 K to 270 K has been observed for CP47, a core antenna complex of photosystem II (Groot et al., 1995).

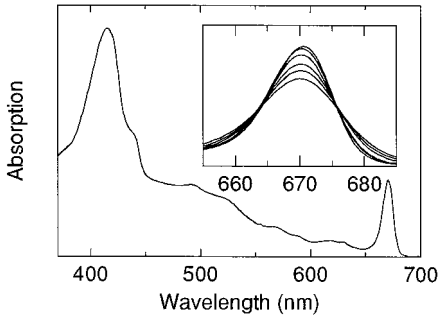

FIGURE 1 Absorption spectrum of air-oxidized $Cytb_6f$ at 4 K. The spectral bandwidth was 1 nm. The inset shows the Chl Q_y-region of the spectrum as a function of temperature. The highest, narrowest spectrum is at 4 K, the lowest and broadest is at 275 K. In between are 50, 100, 175, and 225 K, respectively.

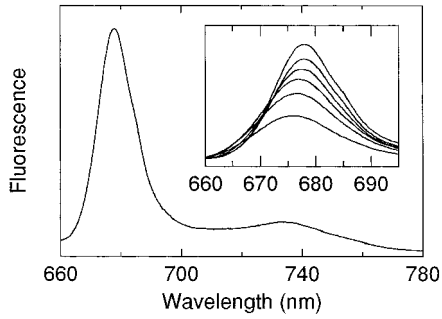

FIGURE 2 Fluorescence emission spectrum of air-oxidized $Cytb_6f$ at 5 K. Excitation was at 455 nm, with a bandwidth of 20 nm. The bandwidth of detection was 1 nm. The inset shows the $(1,0 \rightarrow 0,0)$ region as a function of temperature. The highest, narrowest spectrum is the one at 5 K, the lowest and broadest at 275 K. In between are 50, 100, 175, and 225 K, respectively.

Anisotropy of the emission

The $Cytb_6f$ studied is monomeric. This means that only one Chl molecule is present per complex, if the Chl is bound specifically. If it is bound nonspecifically, one would expect some complexes to bind more than one Chl. Consequently, energy transfer might be possible between the Chl's, leading to a decrease of the anisotropy of the emission. In Fig. 3 examples of polarized emission spectra of $Cytb_6f$ at 5 K, excited at 666 and 676 nm, are shown. At both wavelengths (to the blue and red of the absorption maximum) the emission is highly polarized, the anisotropy is 0.34 ± 0.03 in both cases. Furthermore, upon excitation at other wavelengths in the range from 655 to 684 nm, the anisotropy is

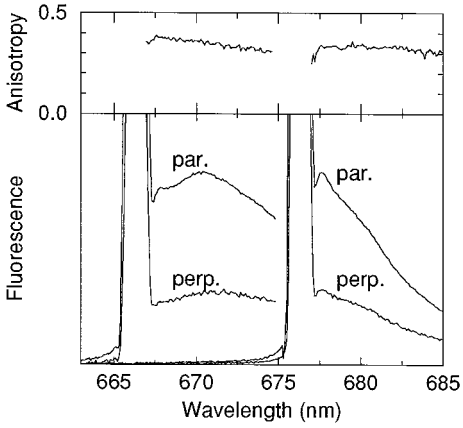

FIGURE 3 Polarized emission spectra of air-oxidized $Cytb_6f$ at 5 K with detection polarized parallel (par.) and perpendicular (perp.) to excitation. The anisotropy is shown in the top panel. Laser excitation was at 666 (*left spectrum*) and 676 nm (*right spectrum*). The bandwidth of detection was 1 nm.

high (~0.34; not shown). The anisotropy of the emission is close to the theoretical maximum (0.4), which is reached if absorption and emission transition dipole moments are parallel. This indicates that no energy transfer takes place between the Chl's in $Cytb_6f$, and strongly suggests that only one Chl is specifically bound per (monomeric) $Cytb_6f$. Further evidence for specific binding will be given below.

Fluorescence quantum yield

We have determined the fluorescence quantum yield of the Chl in $Cytb_6f$ (at room temperature) by comparing the areas of the emission spectrum to that of Chl in methanol. The fluorescence quantum yield of the Chl in $Cytb_6f$ is more than 10 times smaller than that of Chl in methanol. If for the latter a value of 22% is assumed (Seely and Connolly, 1986), the former can be calculated to be 1.8 ± 0.4%. This quantum yield is independent of the redox states of the hemes, which were modified by the consecutive addition of ferricyanide, ascorbate, and dithionite. Interestingly, the fluorescence quantum yield increased to the same value as for Chl in methanol after the addition of Triton X-100 (2% v/v). At such concentrations, the detergent Triton denaturates the protein and removes the Chl from it (Kwa et al., 1994). It should be noted that a decrease in the fluorescence yield of the Chl in dimeric $Cytb_6f$ from *C. rheinhardtii* of a factor of only 4 (compared to Chl in methanol) has been reported (Pierre et al., 1997).

Fluorescence lifetime

We have determined the fluorescence lifetime of $Cytb_6f$ at room temperature, using global analysis of a two-dimensional data set (fluorescence intensity versus time and wavelength) measured with a streak camera. Excitation was at 670 nm and detection in the range of 640–740 nm. In Fig. 4, a time trace of the data (sum of data from 700 nm to 725 nm) is shown, together with fit and residual. The whole data set could be fitted satisfactorily with one decay time: 250 ± 20 ps. This fluorescence lifetime is about a factor of 20 less than that of Chl *a* in a "normal" protein environment or methanol (5–6 ns; Seely and Connolly, 1986), indicating that the Chl is specifically bound. No nanosecond component was needed to fit the data, which indicates that the amount of Chl that is specifically bound to the complex is larger than 95%.

Triplet-minus-singlet measurements

To further study the fate of the Chl excited states, we performed T-S measurements at 77 K. These measurements (not shown) indicate that the yield of Chl triplet formation upon laser flash excitation is very small. It is difficult to determine the triplet yield exactly, but it is at least an order of magnitude smaller than that of Chl in methanol. The difference spectrum (not shown) is a typical Chl T-S spectrum (Hoff, 1986), showing a bleaching of the total absorption spectrum (minima at 670 nm and 436 nm) and excited-state absorption over the whole spectrum (maximum at 460 nm). Furthermore, no transfer of Chl triplets to carotenoids or hemes was observed. The lifetime of the Chl triplets is 2.0 ms, as normally observed for Chl in solution and in a protein environment (Groot et al., 1995; Hoff, 1986). These results, combined with those of the fluorescence lifetimes, show that the lifetime of the singlet excited state of Chl in $Cytb_6f$ is strongly quenched compared to that of Chl in organic solution. This quenching is caused by an increase in the internal conversion rate, or excitation/electron transfer, but not by an increase in the intersystem crossing rate.

Site-selected fluorescence

To obtain information on electron-phonon and vibronic coupling for the Chl in $Cytb_6f$, we recorded fluorescence emission spectra at 5 K upon excitation with a narrow-bandwidth laser. In Fig. 5 some typical spectra are shown, that were measured upon excitation in the range of 660–680

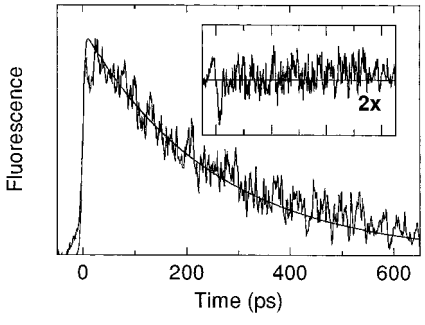

FIGURE 4 Time-resolved fluorescence trace of air-oxidized $Cytb_6f$ at room temperature. Excitation was at 670 nm. Shown is the integrated emission from 700 to 725 nm (*noisy line*) and a monoexponential fit with a decay time of 250 ps. The inset shows the residual of the fit.

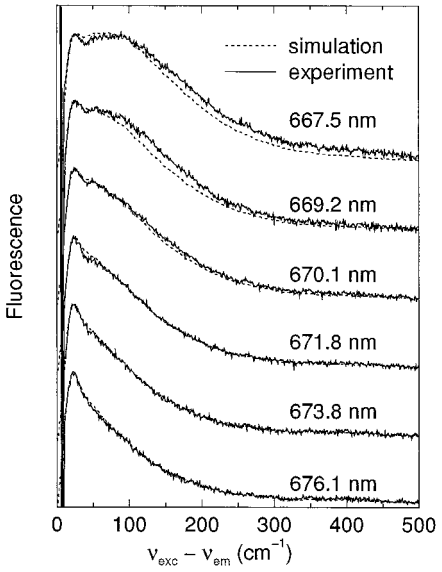

FIGURE 5 Site-selected emission spectra of air-oxidized Cytb$_6$f at 5 K. Shown are experimental (——) and simulated (·····, $S = 0.9$, width IDF 210 cm^{-1}; for details see text) spectra upon (laser) excitation at the indicated wavelengths. The bandwidth of detection was 0.25 nm. The spectra are shown on an energy scale, shifted such that the excitation is at 0 cm^{-1}.

nm (*solid lines*). The spectra are shown on a wavenumber scale and are shifted such that the excitation wavelength corresponds to the origin. In all spectra a sharp peak around 0 cm^{-1} can be seen, which is due to considerable contribution of the zero-phonon line (ZPL) and scattering of excitation light. To the red of this ZPL in all spectra, a relatively broad wing is present. Upon excitation in the extreme red, when only ZPLs are excited, this wing equals the phonon wing (PW) of the single-site spectrum. More to the blue, the Chls are also excited in their PWs, which leads to an apparent larger Stokes shift and broadening of the red wing. Simulations of the excitation wavelength dependence of the site-selected fluorescence spectra are shown below.

Vibronic fine structure upon (1,0 ← 0,0) excitation

Upon narrow-band excitation above 670 nm, narrow lines can be observed in the emission spectra, to the red of the pure electronic ZPL. These narrow lines (vibronic ZPLs, vZPLs) are due to vibronic (1,0 → 0,*x*) transitions without the involvement of phonons. The vZPLs are separated from the pure electronic ZPL with the vibrational frequency of mode *x*. It should be noted that these vZPLs represent vibrations of electronic ground-state Chl. In Fig. 6 *A*, such a line-narrowed emission spectrum is shown. This spectrum was constructed from 18 spectra excited at different wavelengths in the range of 670.9–680.5 nm. The PW of a spectrum excited at 675.4 nm is shown in Fig. 6 *B*. The PW peaks at 25 cm^{-1} to the red of the excitation wavelength. Compared to the PW of the emission of Chl in the reaction center of photosystem II (Peterman et al., in press), the PW is broad and lacks structure. It is more like the PW we reported for LHCII (Peterman et al., 1997). In the vibronic region over 50 vZPLs can be observed. They are listed, together with relative intensities, in Table 1 (in column S_0). Because of the lower quality of the spectrum and the fact that we also needed to add several relatively blue excited spectra to the average spectrum of Fig. 6 *B*, we did not estimate the Franck-Condon factors from the spectra, as we did for LHCII (Peterman et al., 1997). The vibrational frequencies are very similar to those observed with the same technique for Chl *a* in vitro (Avarmaa and Rebane, 1985)

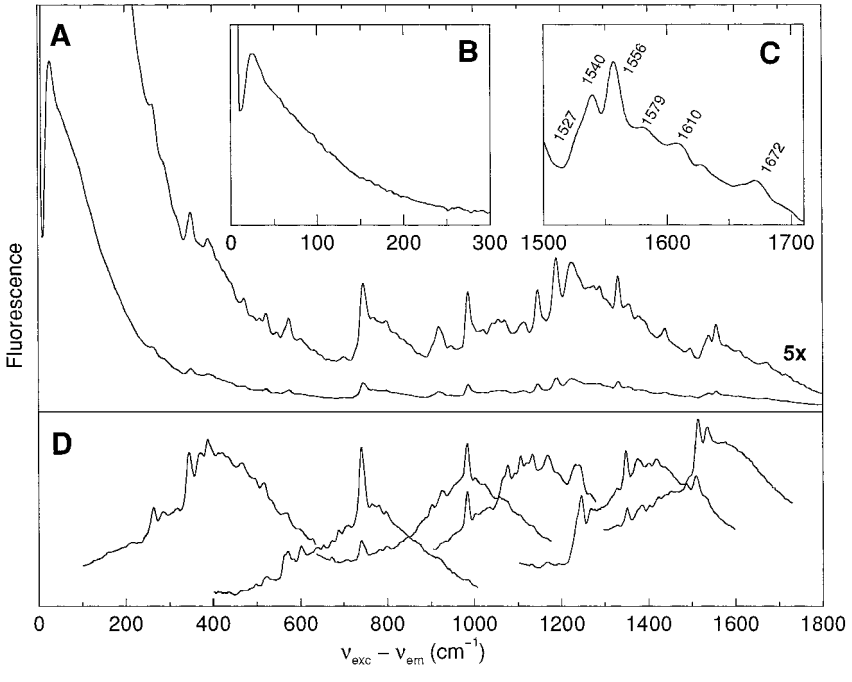

FIGURE 6 Line-narrowed emission spectra of air-oxidized Cytb$_6$f at 5 K. The spectral bandwidth of detection was 0.25 nm. The spectra shown in *A* are excited in the (1,0 ← 0,0) Q_y transition. These spectra are the smoothed average of 18 spectra excited from 670.9 to 680.5 nm. Also shown is a 5× magnification of the vibronic region of the spectrum. *B* shows a magnification of the phonon wing, and *C* a magnification of the 1500–1700 cm^{-1} vibronic region. The spectrum of the phonon wing (*B*) is measured at different conditions: lower OD (0.1) and excitation at 675.4 nm (see text). For the other spectra, a higher OD (0.23 in the Q_y maximum) was used. In *D* emission spectra are shown that are excited in vibronic (1,*x* ← 0,0) Q_y transitions at 656.8, 644.8, 634.8, 628.0, 616.8, and 611.3 nm, going from left to right. The fragments shown of the spectra are due to (1,0 → 0,0) emission. See text for details.

TABLE 1 Vibrational frequencies of Chla in $Cytb_6f$ as obtained from line-narrowed emission spectra recorded at 5 K

S_0		S_1		S_0		S_1		S_0		S_1	
ν (cm^{-1})	Rel. int.	ν (cm^{-1})	Rel. int.	ν (cm^{-1})	Rel. int.	ν (cm^{-1})	Rel. int.	ν (cm^{-1})	Rel. int.	ν (cm^{-1})	Rel. int.
~100	w					673	w			1170	s
124	w					687	w	1189	s	1196	w
263	m	262	s	700	w	708	w	1220	m		
288	m	283	m	725	w			1229	m	1232	w
		318	w	744	s	740	s	1241	m	1245	s
348	m	345	s	750	m	750	m	1264	w	1267	m
		371	s	768	w	766	w	1274	m		
388	m	388	s			781	m	1289	m		
398	m	395	m	797	w	798	m	1303	w		
		412	w			877	w	1331	s	1328	w
		421	w	904	w	901	m	1354	m	1347	s
		436	w	919	m	925	m	1378	w	1375	m
472	m	468	s	946	w			1394	w	1400	w
505	w	497	m	985	s	984	s			1418	m
523	m	519	s	1018	w	1002	m	1438	m	1438	w
547	w	535	s	1040	m			1497	w	1490	w
565	w	564	m	1056	m	1066	w	1527	w	1514	s
574	s	570	s	1070	m	1076	m	1540	s	1534	s
606	w	601	s			1093	w	1556	s		
		623	w	1108	w	1106	s	1579	w		
		638	w	1119	m	1122	w	1610	w		
		653	w	1146	s	1133	s	1672	w		

The ground-state frequencies are obtained from the (1,0 → 0,*x*) vibronic transitions in the spectra excited via the (1,0 ← 0,0) Q_y transition (Fig. 6 *A*). The error margins of these frequencies are ±2 cm^{-1}. The excited-state vibrational frequencies are obtained from the (1,0 → 0,0) emission peaks in the spectra excited via the (1,*x* ← 0,0) Q_y transition (Fig. 6 *D*). The error margins of these frequencies are ±4 cm^{-1}. The relative intensities of the vibronic features are denoted by s (strong), m (medium), and w (weak).

and in other pigment-protein complexes (Peterman et al., 1997, and manuscript submitted for publication). Also with resonance Raman similar frequencies have been observed (Lutz, 1974). Fig. 6 *C* shows the 1500–1700 cm^{-1} vibronic region. In this region, three bands at 1527, 1556, and 1610 cm^{-1} are observed that can be assigned to stretch modes of the methine bridges (Fujiwara and Tasumi, 1986a,b). The frequencies of these three modes indicate that only one axial ligand is bound to the central Mg of the Chl in $Cytb_6f$. For a central Mg with two axial ligands, the frequencies of these modes would be ~10 cm^{-1} lower (Fujiwara and Tasumi, 1986a,b). The band at 1672 cm^{-1} can be assigned to the stretch of the 13^1-keto carbonyl. The frequency of this mode indicates that the 13^1-keto carbonyl accepts a hydrogen bond from the protein environment. A frequency of ~1690 cm^{-1} is expected in the case of an unbound 13^1-keto carbonyl (Lutz and Robert, 1988). The frequencies at 1610 and 1672 cm^{-1} are close to but not identical to those observed with resonance Raman spectroscopy of dimeric $Cytb_6f$ from *C. rheinhardtii* at 77 K (at 1606 and 1676 cm^{-1}) (Pierre et al., 1997). In contrast to our observations, the methine stretch frequency at 1606 cm^{-1} observed for the complex from this algae made an unambiguous assignment of the number of axial ligands based on the Raman spectra impossible in Ref. 6. The difference between these and our results might be a result of the different sample preparations or might be a temperature effect.

Vibronic structure upon (1,*x* ← 0,0) excitation

Upon excitation below ~660 nm (in the vibronic Q_y (1,*x* ← 0,0) region) of the Chl in $Cytb_6f$, fine structure could also be observed (Fig. 6 *D*). This pseudo-line structure in the 660–680-nm region is due to pure electronic ZPLs upon excitation in vZPLs and is shifted with the vibrational frequency from the excitation wavelength (Avarmaa and Rebane, 1985; Kwa et al., 1994). It should be noted that these spectra yield information on vibrations of the Chl in the Q_y excited state. In Fig. 6 *D* some spectra obtained at typical excitation wavelengths are shown. To our knowledge, this is the first time that these kinds of spectra have been reported for Chl *a* in an intact, in vivo protein environment. This kind of fine structure has not been observed for other Chl *a* binding complexes, most probably because most pigment-protein complexes contain several Chl molecules that can exchange excitations. Because of this excitation transfer, site selection is hardly possible (unless upon excitation in the red edge of the (1,0 ← 0,0) Q_y band; Peterman et al., 1997, and manuscript submitted for publication). Electronic excited-state vibrational frequencies obtained from pseudo-lines in spectra measured upon excitation at 14 different wavelengths in the 605–665-nm range are listed in Table 1. Most frequencies are not identical, but are very close to those of the ground-state vibrations. The fact that ground- and Q_y-excited-state vibrational frequencies are so similar suggests that the shapes of the potential

energy surfaces of the two states do not differ substantially. Unfortunately, the 1550–1700 cm^{-1} vibrations could not be observed. An explanation for the absence of these vibrations might be that at the wavelengths at which these are excited (~600 nm), the background of nonselective excitation (for example, in the Q_x) is too large to observe fine structure. The excited-state vibrational frequencies of Chl in $Cytb_6f$ are very similar to those measured for Chl in organic solvent (Avarmaa and Rebane, 1985) and detergent solution (Kwa et al., 1994) by the same technique.

Simulations of the site-selected fluorescence spectra

The dotted spectra in Fig. 5 are simulations of the site-selected emission spectra. These simulations have been performed as described before (Peterman et al., in press). In short, the PW of the red excited emission spectrum of Fig. 6 *B* is used ($Em_{red}(\nu)$) as a single-site fluorescence spectrum ($Em_{SS}(\nu)$). Instead of the experimental ZPL (which is contaminated with scatter), a delta function ($\delta(\nu)$, normalized to unit area) is used. As single-site absorption spectrum ($Abs_{SS}(\nu)$), the mirror image of $Em_{SS}(\nu)$ (with respect to wavenumbers), is used. The strength of the electron-phonon coupling, as expressed in the Huang-Rhys factor *S*, is included in these single-site spectra as the relative area of ZPL and PW:

$$Em_{SS}(\nu) = \delta(\nu) + \left\{\frac{e^{+S} - 1}{\int_{-500}^{0} Em_{red}(\nu) \cdot d\nu}\right\} \cdot Em_{red}(\nu) \qquad (1)$$

Here we have made the somewhat arbitrary assumption that the PW extends up to 500 cm^{-1} from the ZPL. A Gaussian is used for the IDF. The parameters of the Gaussian are chosen such that the experimental absorption spectrum is optimally simulated. The site-selected emission spectra ($Em(\nu, \nu_{exc})$) excited at ν_{exc} are calculated with

$$Em(\nu, \nu_{exc}) = \int_{-\infty}^{\infty} Em_{SS}(\nu - \omega) \cdot Abs_{SS}(\nu_{exc} - \omega) \cdot IDF(\omega) \cdot d\omega \qquad (2)$$

The best agreement of simulated and experimental site-selected emission spectra is obtained with a value for *S* of 0.9 ± 0.2 and a width of 210 ± 10 cm^{-1} for the IDF, which peaks at 672.0 nm (Fig. 5). It should be noted that these parameters are chosen such that the (5 K) absorption spectrum is reproduced satisfactorily. With these parameters, the (5 K) nonselective (excited at 455 nm) emission spectrum cannot be simulated reasonably. Both the Stokes shift (simulation: 3 nm; experiment: 7.5 nm (peak-to-peak)) and the width (simulation: 11.4 nm; experiment: 15.3 nm (FWHM)) are underestimated. See below for an explanation of this discrepancy.

Simulations of the temperature dependence of the absorption and emission spectra

We have simulated the temperature dependence of both absorption (Fig. 1) and nonselectively excited (at 455 nm) emission spectra (Fig. 2), using an algorithm based on linear, harmonic, Franck-Condon electron-phonon coupling and a temperature-independent IDF. This algorithm has been described extensively elsewhere (Pullerits et al., 1995). It has been applied before on B820 (the subunit of purple bacterial light-harvesting complex I) and LHCII (Peterman et al., 1997). The simulations yield values for the electron-phonon coupling strength *S* and the width of the IDF. The input for the simulations is the PW obtained from a red-excited site-selected emission spectrum (Fig. 6 *B*). From this PW a so-called one-phonon profile of the electronic transition can be calculated (Kukushkin, 1965). This one-phonon profile is the spectrum of the one-phonon transitions coupled to the electronic transition. In optical response theory it is known as the real part of the spectral density (Mukamel, 1995) and contains information on the environment of the pigment and the vibrational modes of the pigment itself. The unknown parameter here is the Huang-Rhys factor, *S*. By making an initial guess at *S*, the temperature dependence of the homogeneous spectra can be simulated. For a good comparison of the simulated spectra with the experimental ones, inhomogeneous broadening also has to be accounted for. This is included by assuming a temperature-independent Gaussian inhomogeneous distribution function. In optical response theory this corresponds to the imaginary part of the spectral density (Mukamel, 1995). Comparison with experiment is carried out via the second moment of the red (absorption) or blue (emission) part of the spectrum. The results are shown in Fig. 7. A good simulation of the temperature dependence of the absorption

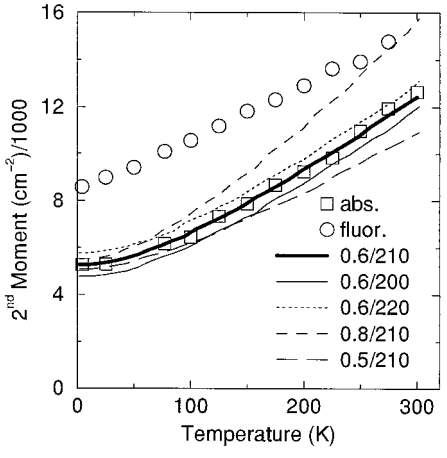

FIGURE 7 Simulations of the temperature dependence of the second moments of absorption and emission spectra of air-oxidized $Cytb_6f$. The experimental data points are indicated by squares (absorption) and circles (emission, excited at 455 nm). Simulations are shown for different values of *S* (0.5, 0.6, and 0.8) and of the width of the IDF (200, 210, and 220 cm^{-1}) as indicated. For details of the simulation procedure, see text.

spectrum is obtained when S is taken to be 0.6 ± 0.05, and the width of the IDF to be 210 ± 10 cm^{-1}. A remarkable observation for LHCII was that up to 200 K, the broadening of the absorption band could be simulated rather well, but that above this temperature the experimental broadening strongly deviated. It was suggested that this is due to some sort of phase transition in the protein (Peterman et al., 1997). For $Cytb_6f$ we do not observe a similar breakdown of the simulation, which might suggest that the structure of this complex is more rigid at higher temperatures.

The temperature dependence of the second moment of the blue side of the nonselectively excited fluorescence spectrum (excitation at 455 nm; Fig. 7) cannot be simulated with the same width of the IDF (in contrast to the selectively excited fluorescence spectra; see above). However, the slope of the broadening suggests roughly the same value for S as for absorption. Technically we could get a fit to these fluorescence broadening data by assuming that the IDF has broadened to ~270 cm^{-1} upon excitation in the blue. Excitation in the blue might provide access to additional states in the configurational space of the Chl environment and might in that way broaden the IDF. Another explanation could be that after internal conversion from Soret to Q_y, the Chl molecule becomes locally hot. In this respect, we remark that the fluorescence data do not show the typical plateau up to ~50 K (compare to the absorption in Fig. 7), which supports this idea. Furthermore, it should be noted that the lifetime of the Chl excited state is rather short, possibly too short for total cooling of the Chl environment to take place. We could superimpose fluorescence and absorption data by shifting the former by ~150 K toward higher temperature. This would mean that the excess energy (~7000 cm^{-1}) is distributed among ~70 modes ($k \cdot \Delta T$ = ~100 cm^{-1}). This appears to be too small a number for a system with so many degrees of freedom as a Chl-protein complex. In reality, most likely both broadening of the IDF and local heating take place. These phenonena might also be the cause of the large Stokes shift of the emission.

Two different analysis methods have led to the same value of the width of the inhomogeneous distribution, 210 ± 10 cm^{-1}. The values obtained for S with these methods (0.6 ± 0.05 and 0.9 ± 0.2) are slightly different. However, given the error margins and the assumptions of both methods, the values agree reasonably well.

DISCUSSION

We have presented an extensive characterization of the absorption and fluorescence properties of the Chl in monomeric $Cytb_6f$ of *Synechocystis PCC6803*. The purified complexes bind essentially one Chl per complex, and we have shown that both fluorescence yield and lifetime are more than an order of magnitude smaller than those of Chl *a* in methanol and after the addition of TX-100 to the $Cytb_6f$ sample. These results indicate that our preparation is virtually devoid of adventituously bound Chl, and that the Chl must be present in a well-defined protein environment. Using high-resolution fluorescence spectroscopy, we have identified over 50 vibrational frequencies in both the ground and the Q_y excited states. These vibrational frequencies of the Chl indicate that one axial (protein) ligand binds to its central magnesium and confirm that its 13^1-keto carbonyl accepts a hydrogen bond (as observed for the complex of *C. rheinhardtii*; Pierre el al., 1997). We have simulated both the temperature dependence of the absorption and emission spectrum and the site-selected fluorescence spectra. From these simulations we have obtained values for the strength of the electron-phonon coupling (S = 0.6–0.9) and the width of the IDF (210 ± 10 cm^{-1}). From the fluorescence anisotropy we have concluded that only one Chl is specifically bound per (monomeric) $Cytb_6f$ complex. Our results do not provide clues to the function of the Chl, but indicate how the Chl is "tolerated" (see below).

Some of our spectroscopic observations (fluorescence yield, ground-state vibrational frequencies) of the Chl in $Cytb_6f$ of *Synechocystis* are different from those measured before for the complex of *C. rheinhardtii* (Pierre et al., 1997). It is unclear whether this is due to the differences in measuring methods or is intrinsic to the different preparations. Our monomeric $Cytb_6f$ from *Synechocystis* does not contain the Fe-S cluster; the complex isolated from *C. rheinhardtii* (Pierre et al., 1997) was dimeric, contains the Fe-S cluster, and was isolated with a different detergent. We note that a small contamination with (highly fluorescing) nonspecifically bound Chl can severely contaminate the steady-state fluorescence spectra.

The only spectroscopic characteristics of Chl in $Cytb_6f$ that clearly differ from Chl in (organic or detergent) solution are the short lifetime (250 ± 20 ps, only 5.0 ± 0.4% of that of Chl in methanol; Seely and Connolly, 1986), the low fluorescence quantum yield (1.8 ± 0.4%, only 8 ± 2% of that of Chl in methanol), and the low triplet yield. These results show that the lifetime of the Q_y (singlet) excited state of Chl in $Cytb_6f$ is shortened by a factor of ~20. The fluorescence quantum yield suggests somewhat less shortening of the excited-state lifetime than the fluorescence lifetime measurements. This can be explained by a small contamination of unbound Chl, which raises the quantum yield slightly, but does not influence the 250-ps lifetime observed in the fluorescence lifetime measurements. The numbers suggest a contribution of unbound Chl of 32 ± 22% to the steady-state emission spectra. However, we did not observe an excitation wavelength dependence of the vibronic details of the line-narrowed fluorescence spectra. This could be expected if two different pools of Chl would contribute. The absence of this effect suggests that the contribution of unbound Chl is small (less than ~20%), or that there is no spectral difference between bound and unbound Chl.

The quenching of the singlet excited state supports the idea that the Chl binds to a specific binding pocket of the $Cytb_6f$ complex. It is of key importance to the organism to keep the amount of Chl triplet states as low as possible. Chl

triplet states can sensitize molecular oxygen. In this process singlet excited oxygen is formed, which is a reactive, oxidizing agent that is harmful to the organism (Siefermann-Harms, 1987). In photosynthesis the formation of singlet oxygen is normally prevented by quenching of Chl triplets by carotenoids (Siefermann-Harms, 1987). This mechanism is not functioning in $Cytb_6f$, despite the presence of Cars. In this complex the singlet oxygen problem is solved in a different way: the Chl singlet excited state is substantially quenched, which leads to a pronounced decrease in the quantum yield of Chl triplet formation.

We can only speculate about the exact mechanism of this quenching process. There is evidence that the Chl is bound to the cytochrome b6 protein (Poggese et al., 1997). It might be that the b6 heme or one of the other hemes accepts the Chl excitation via excitation or electron transfer. If (one of) the hemes were responsible for the quenching, one might expect an effect of the redox states of the hemes on the fluorescence yield. We have shown that there is no such effect. The quenching might also proceed via another mechanism. A mechanism that is well known for flavin-binding proteins is quenching of a chromophore excited state by specific amino acids (aromatic ones and cysteine) that are in close contact with the chromophore, via electron or charge transfer (Visser et al., 1987). In several flavin-binding proteins that are involved in electron transfer (in these proteins, the flavin is a redox cofactor and fluorescence is functionally not important), flavin fluorescence is quenched 20- to 100-fold via this mechanism (Visser et al., 1987). In other complexes involved in bioluminescence, for which fluorescence is of functional importance, the binding pocket of the flavin is optimized in such a way (rigid, no cysteine and aromatic amino acids) that the fluorescence yield is large (Visser et al., 1997). It is unknown whether aromatic amino acids or cysteine can also quench Chl excited states. However, it has been suggested that in the water-soluble bacteriochlorphyll a complex of green bacteria, bacteriochlorophyll excited states can be quenched by radicals from amino acid residues like tyrosine (Li et al., 1997). The parallel with the flavin-binding proteins of adjusting the excited state lifetime of the cofactor for optimal functioning by modifying its binding site is an interesting one. In most Chl-binding complexes (involved in light-harvesting or energy conversion) it is essential to minimize singlet excited-state quenching. It is suggested that the Chl excited state in $Cytb_6f$ has no functional role (Pierre et al., 1997). However, the potentially harmful formation of Chl triplets has to be avoided. If the (singlet) excited state of Chl has no function, this is most easily achieved by substantially shortening the lifetime. We propose that in $Cytb_6f$ the Chl binding pocket is modified in such a way that it is optimal for quenching of the Chl singlet excited state. If the Chl in $Cytb_6f$ is indeed a evolutionary relic (Pierre et al., 1997), the presence of this Chl in a strongly quenching environment (which makes it harmless) might explain the lack of evolutionary pressure to lose the Chl.

We thank René Monshouwer, Bas Gobets, and Wouter Abbestee for help with the streak-camera measurements, and Dr. Ivo van Stokkum for help with the global analysis of the time-resolved fluorescence data. We thank Dr. Bruno Robert for discussion.

This work was supported by the Netherlands Foundation for Scientific Research (NWO) via the Foundation for Life Sciences (SLW) and the European Union (contract numbers 94 0619 and 93 0361 to L-OP). The financial support by the Deutsche Forschungsgemeinschaft (grant Ro 858/2-3) is gratefully acknowledged (MR).

REFERENCES

Avarmaa, R. A., and K. K. Rebane. 1985. High-resolution optical spectra of chlorophyll molecules. *Spectrochim. Acta.* 41A:1365–1380.

Bald, D., J. Kruip, E. J. Boekema, and M. Rögner. 1992. Structural investigations on cyt b6/f-complex and PSI-complex from the cyanobacterium *Synechocystis* PCC6803. *In* Photosynthesis: From Light to Biosphere, Part I. N. Murata, editor. Kluwer Academic Publishers, Dordrecht, the Netherlands. 629–633.

Breyton, C., C. Tribet, J. Olive, J. P. Dubacq, and J. L. Popot. 1997. Dimer to monomer conversion of the cytochrome b6f complex—causes and consequences. *J. Biol. Chem.* 272:21892–21900.

Cramer, W. A., G. M. Soriano, M. Ponomarev, D. Huang, H. Zhang, H. E. Martinez, and J. L. Smith. 1996. Some new structural aspects and old controversies concerning the cytochrome b6f complex of oxygenic photosynthesis. *Annu. Rev. Plant Physiol. Plant Mol. Biol.* 47:477–508.

Dawson, R. M. C., D. C. Elliot, W. H. Elliot, and K. M. Jones. 1986. Data for Biochemical Research. Clarendon Press, Oxford. 232–233.

Fujiwara, M., and M. Tasumi. 1986a. Resonance Raman and infrared studies on axial coordination to chlorophylls a and b in vitro. *J. Phys. Chem.* 90:250–255.

Fujiwara, M., and M. Tasumi. 1986b. Metal-sensitive bands in the Raman and infrared spectra of intact and metal substituted chlorophyll *a*. *J. Phys. Chem.* 90:5646–5650.

Groot, M. L., E. J. G. Peterman, I. H. M. van Stokkum, J. P. Dekker, and R. van Grondelle. 1995. Triplet and fluorescing states of the CP47 antenna complex of photosystem II studied as function of temperature. *Biophys. J.* 68:281–290.

Hauska, G., M. Schütz, and M. Büttner. 1996. The cytochrome b6f complex—composition, structure and function. *In* Oxygenic Photosynthesis: The light Reactions. D. R. Ort and C. F. Yocum, editors. Kluwer Academic Publishers, Dordrecht, the Netherlands. 377–398.

Hoff, A. J. 1986. Triplets: phosphorescence and magnetic resonance. *In* Light Emission by Plants and Bacteria. Govindjee, J. Amesz, and D. C. Fork, editors. Academic Press, New York. 225–265.

Huang, D., R. M. Everly, R. H. Cheng, J. B. Heymann, H. Schägger, V. Sled, T. Ohnishi, T. S. Baker, and W. A. Cramer. 1994. Characterization of the chloroplast cytochrome b6f complex as a structural and functional dimer. *Biochemistry.* 33:4401–4409.

Kukushkin, L. S. 1965. Reciprocal problems for certain processes related to multiphonon transitions. *Soviet Phys. Solid State.* 7:38–43.

Kwa, S. L. S., S. Völker, N. T. Tilly, R. van Grondelle, and J. P. Dekker. 1994. Polarized site-selection spectroscopy of chlorophyll *a* in detergent. *Photochem. Photobiol.* 59:219–228.

Li, Y. F., W. L. Zhou, R. E. Blankenship, and J. P. Allen. 1997. Crystal structure of the bacteriochlorophyll a protein from *Chlorobiom tepidum*. *J. Mol. Biol.* 271:456–471.

Lutz, M. 1974. Resonance Raman spectra of chlorophyll in solution. *J. Raman Spectrosc.* 2:497.

Lutz, M., and B. Robert. 1988. Chlorophylls and photosynthetic membrane. *In* Biological Applications of Raman Spectroscopy. T. G. Spiro, editor. Wiley, New York. 347–411.

Metzger, S. U., W. A. Cramer, and J. Whitmarsh. 1997. Critical analysis of the extinction coefficient of chloroplast cytochrome f. *Biochim. Biophys. Acta.* 1319:233–241.

Mukamel, S. 1995. Principles of Nonlinear Optical Spectroscopy. Oxford University Press, New York.

Personov, R. I. 1983. Site-selection spectroscopy of complex molecules in solutions and its applications. *In* Spectroscopy and Excitation Dynamics

of Condensed Molecular Systems. V. M. Agranovich and R. M. Hochstrasser, editors. North Holland, Amsterdam. 555–619.

Peterman, E. J. G., T. Pullerits, R. van Grondelle, and H. van Amerongen. 1997. Electron-phonon coupling and vibronic fine structure of light-harvesting complex II of green plants: temperature dependent absorption and high-resolution fluorescence spectroscopy. *J. Phys. Chem. B.* 101: 4448–4457.

Peterman, E. J. G., H. van Amerongen, R. van Grondelle, and J. P. Dekker. 1998. The nature of the excited state of the reaction center of photosystem II of green plants: A high-resolution fluorescence spectroscopy study (fluorescence line narrowing/chlorophyll a). *Proc. Natl. Acad. Sci. USA*. 95: in press.

Pierre, Y., C. Breyton, D. Kramer, and J. L. Popot. 1995. Purification and characterization of the cytochrome b6f complex from *Chlamydomonas reinhardtii. J. Biol. Chem.* 270:29342–29349.

Pierre, Y., C. Breyton, Y. Lemoine, B. Robert, C. Vernotte, and J. L. Popot. 1997. On the presence and role of a molecule of chlorophyll a in the cytochrome b6f complex. *J. Biol. Chem.* 272:21901–21908.

Poggese, C., P. Polverino de Laureto, G. M. Giacometti, F. Rigoni, and R. Barbato. 1997. Cytochrome b6f complex from the cyanobacterium *Synechocystis* 6803: evidence of dimeric organization and identification of chlorophyll-binding subunit. *FEBS Lett.* 414:585–589.

Pullerits, T., R. Monshouwer, F. van Mourik, and R. van Grondelle. 1995. Temperature dependence of electron-vibronic spectra of photosynthetic systems. Computer simulations and comparison with experiment. *Chem. Phys.* 194:395–408.

Rögner, M., P. J. Nixon, and B. A. Diner. 1990. Purification and characterization of photosystem I and photosystem II core complexes from wild-type and phycocyanin-deficient strains of the cyanobacterium *Synechocystis* PCC6803. *J. Biol. Chem.* 265:6189–6196.

Seely, G. R., and J. S. Connolly. 1986. Fluorescence of photosynthetic pigments in vitro. *In* Light Emission by Plants and Bacteria. Govindjee, J. Amesz, and D. C. Fork, editors. Academic Press, New York. 99–133.

Siefermann-Harms, D. 1987. The light-harvesting and protective functions of carotenoids in photosynthetic membranes. *Physiol. Plantarum*. 69: 561–568.

Van Stokkum, I. H. M., T. Scherer, A. M. Brouwer, and J. W. Verhoeven. 1994. Conformatianol dynamics of flexibly and semirigidly bridged electron donor acceptor systems as revealed by spectrotemporal parametrization of fluorescence. *J. Phys. Chem.* 98:852–866.

Visser, A. J. W. G., A. van Hoek, T. Kulinski, and J. Le Gall. 1987. Time-resolved fluorescence studies of flavodoxin. *FEBS lett.* 224: 406–410.

Visser, A. J. W. G., A. van Hoek, N. V. Visser, Y. Lee, and S. Ghisla. 1997. Time-resolved fluorescence study of the dissociation of FMN from the yellow fluorescence protein from *Vibrio fischeri. Photochem. Photobiol.* 65:570–575.

Xia, D., C. A. Yu, H. Kim, J. Z. Xian, A. M. Kachurin, L. Zhang, L. Yu, and J. Deisenhofer. 1997. Crystal structure of the cytochrome bc1 complex from bovine heart mitochondria. *Science.* 277:60–66.